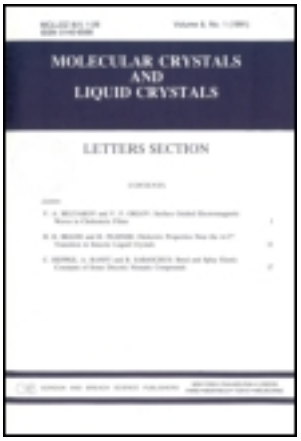

Molecular Crystals and Liquid Crystals
Publication details, including instructions for authors and subscription information:
http://www.tandfonline.com/loi/gmcl20

Physical Properties of ZnSe Thin Films Depending on the Process Parameters

Maeng Jun Kim [a] , Sung Ho Lee [b] , Hong Tak Kim [c] & Sang Ho Sohn [d]

[a] Research Institute for Solar and Sustainable Energies , Gwangju institute of Science and Technology , Gwangju , 500-712 , Republic of Korea

[b] Department of Materials & Energy Engineering , Kyungwoon University , Gumi , 730-739 , Republic of Korea

[c] School of Display and Chemical Engineering , Yeungnam University , Gyeongsan , 712-749 , Republic of Korea

[d] Department of Physics , KyungPook National University , Daegu , 702-701 , Republic of Korea

Published online: 08 Jan 2014.

To cite this article: Maeng Jun Kim , Sung Ho Lee , Hong Tak Kim & Sang Ho Sohn (2013) Physical Properties of ZnSe Thin Films Depending on the Process Parameters, Molecular Crystals and Liquid Crystals, 586:1, 129-137, DOI: 10.1080/15421406.2013.853501

To link to this article: http://dx.doi.org/10.1080/15421406.2013.853501

Mol. Cryst. Liq. Cryst., Vol. 586: pp. 129–137, 2013

ISSN: 1542-1406 print/1563-5287 online
DOI: 10.1080/15421406.2013.853501

Taylor & Francis
Taylor & Francis Group

Physical Properties of ZnSe Thin Films Depending on the Process Parameters

MAENG JUN KIM,[1] SUNG HO LEE,[2,*] HONG TAK KIM,[3] AND SANG HO SOHN[4,*]

[1]Research Institute for Solar and Sustainable Energies, Gwangju institute of Science and Technology, Gwangju 500-712, Republic of Korea
[2]Department of Materials & Energy Engineering, Kyungwoon University, Gumi, 730-739, Republic of Korea
[3]School of Display and Chemical Engineering, Yeungnam University, Gyeongsan 712-749, Republic of Korea
[4]Department of Physics, KyungPook National University, Daegu 702-701, Republic of Korea

ZnSe thin films were grown by a co-evaporation method with various Se/Zn flux ratios. In order to characterize ZnSe thin films, we performed an investigation that utilized X-Ray Diffraction (XRD), Scanning Electron Microscopy (SEM), and Ultra Violet–Visible-Near InfraRed (UV-VIS-NIR) measurements of the structural, optical, and morphological properties. XRD pole-figure analysis confirmed that the orientation of the ZnSe cubic (111) plane has been widely distributed throughout the ψ axis with respect to process conditions, flux rate of Se. It has been found that as long as the Se/Zn flux ratio is larger than 1.43, stable, single-phase, ZnSe thin films can be grown. Additional experimental data revealed that optical properties strongly depend on the substrate temperature and have correlation with crystallinity.

Keywords ZnSe; co-evaporation; characterization

Introduction

There are plenty of application field to To date there are various deposition method to fabricate ZnSe thin films [1–5]. Recent extensive studies for the development of II-VI blue light-emitting diodes (LEDs) or blue laser diodes (LDs) show very significantly the demand for high quality ZnSe single crystals as a substrate for homoepitaxial growth. The ZnSe formation mechanisms from the two elemental materials, Zn and Se, have been studied in earlier reports [6]. To date, the precursor model is perhaps the most substantial explanation of the formation of the ZnSe phase in the co-evaporation deposition method. The precursor model splits the growth process into two steps, physisorption when the atoms are loosely bound to the surface, the precursor state, followed by chemisorption from that state into a site on the growing surface. Desorption can occur from either the precursor state or the surface. According to the precursor model, two reconstructions have been observed on the

*Address correspondence to Prof. Sang Ho Sohn, Department of Physics, Kyungpook National University, Sangyuk-dong, Buk-gu, Daegu 702-701, Korea (ROK). Tel.: (+82)53-950-5892; Fax: (+82)53-950-6893. E-mail: shsohn@knu.ac.kr

Table 1. Se flux rate and Se/Zn flux ratio with respect to effusion cell temperatures

Se Effusion cell temperature (°C)	100	105	110	115	120	125
Deposition rate read by QCM (Å/sec)	2.2	4.1	5.35	6.8	8.3	9.8
Se/Zn flux ratio	1.54	2.88	3.74	4.75	5.80	6.85

ZnSe surface, (2 × 1) Selenium rich and c(2 × 2) Zn rich surfaces. It was expected that the c(2 × 2) would also be a dimerised Zn surface but it was in fact a half-monolayer of Zn atoms bonded to two Se atoms in the next layer with one dangling bond [7–8]. The reported values of the sticking coefficients for Zn and Se during MBE growth of ZnSe are about 0.65 and 0.57 respectively for a substrate temperature of 300°C. These studies reported the sticking coefficients over a wide range of substrate temperatures and flux ratios. In earlier works, it is demonstrated that both Zn and Se are desorbed from the surface over a wide range of temperatures, leading to sticking coefficients much lower than 1.

In this paper, we have deposited ZnSe thin films via the co-evaporation method and performed a comparative study of the optical, structural, and morphological properties of the ZnSe films with respect to various deposition conditions.

Experimental Setup

For characterizing a thin film ZnSe layer, a variety of ZnSe on soda-lime glass substrates were prepared using the co-evaporation method. In the fabrication process for obtaining ZnSe films, the substrate temperatures were detected by a pyrometer, providing a non-contact temperature sensing method with an infrared laser throughout the deposition. The flux rates of Zn and Se from the effusion cell were constantly maintained with a thickness monitor and controlled by the effusion cell heater. In this study, the direct measurement of flux rate was not obtained by using laser spectroscopy method or ion gauge etc. Quartz crystal monitor (QCM) was utilized in order to maintain "flux rate" constantly by monitoring "deposition rate" which QCM sensor actually can read.

The Zn effusion cell temperature was static at 380°C. The Se effusion cell temperature varied from 100 to 125°C with a 5°C gap. Structural properties of ZnSe films were investigated using XRD (Philips X'Pert PRO MPD X-Ray Diffractometer) with a primary wavelength of Cu-Kα_1 1.5406 Å via Bragg-Brentano geometry. Philips X'Pert PRO MRD 4 axis X-Ray Diffractometer was also used for the observation of pole figure analysis. Optical transmittance measurement was obtained by utilizing the Ultra Violet–Visible-Near InfraRed spectrometer (UV-VIS-NIR, Perkin Elmer Lambda 950 model). The surface roughness was measured by using Atomic Force Microscopy (AFM, Digital instruments NanoScope III) in the tapping mode while the surface morphology was investigated by Scanning Electron Microscopy (SEM, Hitachi S-4800 model).

Results and Discussion

The Se flux rate and Se/Zn flux ratio with respect to the effusion cell temperature are listed in Table 1. All experiments were performed at the substrate temperature of 400°C. The Zn deposition rate at 380°C was static, 1.43 Å/sec is within typically 0.5% error which is dependent on process conditions, especially sensor location, material stress, temperature and density.

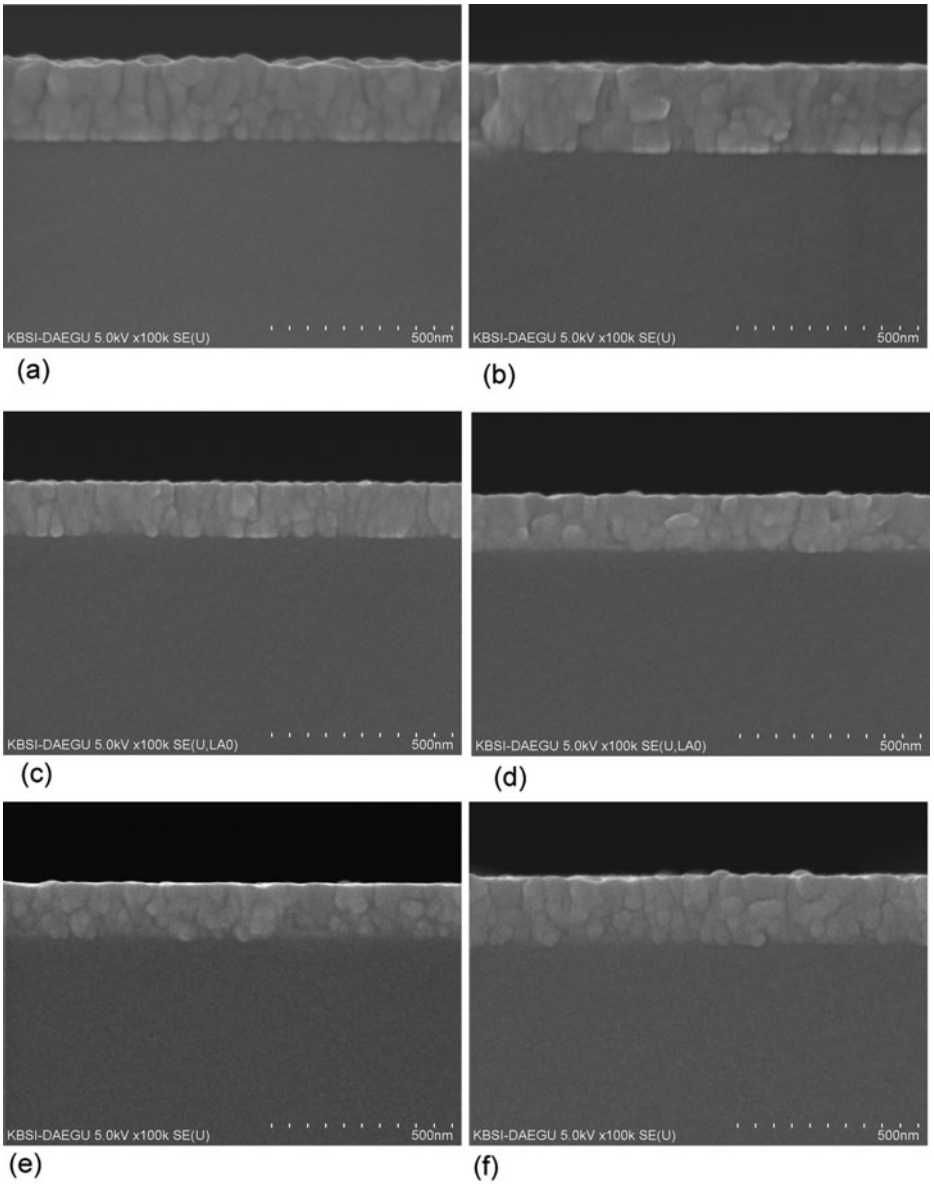

Figure 1. SEM microscopy of ZnSe thin films, with respect to the Se effusion cell temperature. (a) 100°C, (b) 105°C, (c) 110°C, (d) 115°C, (e) 120°C and (f) 125°C, respectively.

Figure 1 represents the cross sectional SEM microscopy of ZnSe thin films with respect to the Se effusion cell temperature. As shown in Fig. 1, the film thicknesses are varying depending on the effusion cell temperatures. The thickness are revealed as 225 nm for 100°C and 105°C, 150 nm for 110°C, 115°C and 120°C, 190 nm for 125°C, respectively. In other words, the thickness of ZnSe thin films depending on the effusion cell temperatures are not monotonic behavior and comprise three different regions.

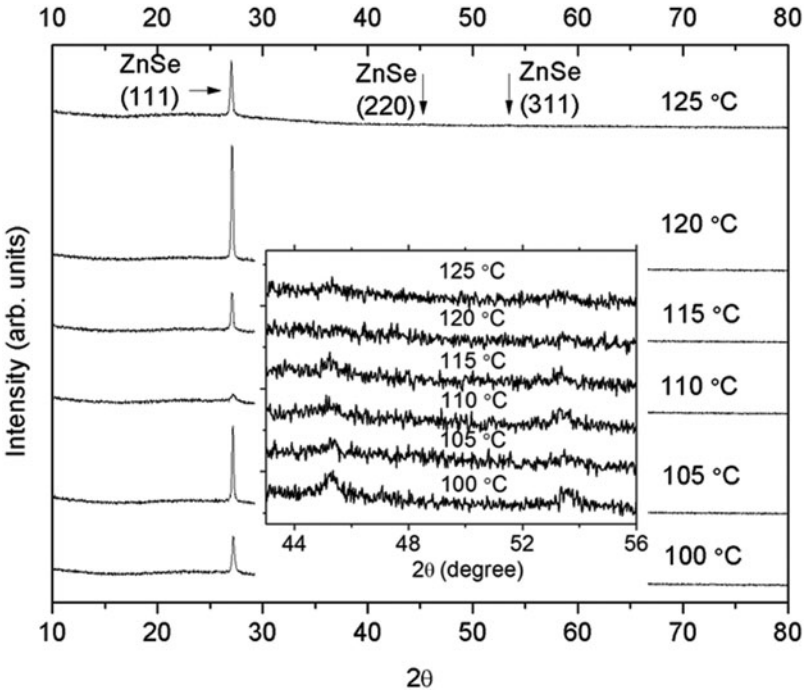

Figure 2. XRD data of ZnSe thin films as a function of effusion cell temperatures.

Many research groups have studied ZnSe surface phase diagram by using molecular beam epitaxy (MBE). The results show that the range of substrate temperature and Se/Zn flux ratio corresponding to specific phase is varying due to equipment geometry and measurement technique. However their common results include that the surface phase diagram can be divided into three major sections. The three parts of the phase diagram showing different surface structures are the Se-rich (2 × 1), the Zn-rich c(2 × 2) ZnSe (001) reconstructions and a mixed region consisting a combination of both as shown described in [10]. Therefore based on prior investigation the peculiar behavior of ZnSe thickness may be due to different surface reconstructions, i.e. the conditions 100°C and 105°C are part of the Zn-rich c(2 × 2), 110°C and 115°C are part of mixed state and 120°C and 125°C are part of the Se-rich (2 × 1) phase reconstruction.

Figure 2 represents the XRD data for ZnSe thin films with respect to the effusion cell temperature and Table 2 is a guide to the quantitative information on XRD peaks according to Fig. 2. The peak seen at 27.2° is associated with the cubic (111) plane while the peaks at 45.24° and 53.24° are associated with the cubic (220) and (311) planes, respectively. As shown in Table 2 with respect to effusion cell temperatures, the quantitative peak information on the cubic (111), (220) and (311) crystal planes differ significantly. These results are similar to SEM data, not monotonic behavior as effusion cell temperature increases. These phenomena can also deduced from the three parts of the phase diagram showing different surface structures. In order to analyze this data with respect to preferred orientation, the pole-figure of ZnSe thin films at the cubic (111) plane has been measured.

Figure 3 represents the pole-figure of ZnSe thin films at the cubic (111) plane depending on the selenium effusion cell temperatures. In X-ray diffraction analysis, the texture is determined from the set of pole-figures. These pole-figures are measured by recording

Table 2. Quantitative information of XRD peaks according to Fig. 2

Se Effusion Cell Temperature (°C)	Peak Information	Crystal Plane		
		C(111)	C(220)	C(311)
100	FWHM	0.25	0.6	0.53
	Intensity	1252	67	51
	Area	285	35	24
105	FWHM	0.16	0.14	None
	Intensity	2551	28	
	Area	409	5	
110	FWHM	0.63	0.25	0.60
	Intensity	223	18	46
	Area	121	4	25
115	FWHM	0.21	0.6	0.21
	Intensity	1312	38	23
	Area	255	21	5
120	FWHM	0.17	None	None
	Intensity	3867		
	Area	640		
125	FWHM	0.23	None	None
	Intensity	1893		
	Area	395		

the intensity distribution of a single (hkl) reflection by tilting and rotating the sample over the orientation sphere, as shown in Figure 4. Using this method, the orientation distribution of a single reflection and thus for a single lattice plane is determined. The angles of conventional XRD pole-figure analysis as represented in Fig. 4 are defined as follows: ω–angle between incident x-rays and sample surface, 2θ–angle between incident x-rays and detector, ψ–sample tilt and ϕ–in-plane sample rotation. The most familiar XRD analysis method, Bragg-Brentano geometry (θ-2θ) measurement (ex. Fig. 2), only shows the diffraction pattern out of the sample surface at $\psi = \phi = 0^\circ$. In our pole-figure analysis of ZnSe (111), the scanning range of ψ and ϕ is 0 to 81° and 0 to 360° respectively.

Because pole figure data reveals ϕ symmetry behavior, the cross-section of Fig. 3 at $\phi = 24^\circ$ (arbitrary choice) with various Se effusion cell temperatures was exhibited as shown in Figure 5. the orientation distribution of ZnSe (111) with respect to the ψ axis shows that for a temperature of 120°C, the most highly concentrated position is at $\psi = 0^\circ$ as expected. However contrary to that case, at a temperature of 110°C, far from being concentrated at $\psi = 0^\circ$, the highest intensity is near $\psi = 60^\circ$. This implies that the 60° tilted cubic (111) crystal plane is most dominant within ZnSe thin films rather than out of the sample plane (0° tilted). In addition, throughout the whole ψ range of 110°C, a flat distribution is revealed. This suggests a wide orientation distribution of cubic (111) crystal plane with respect to the ψ-axis. Therefore, although Bragg-Brentano geometry (θ-2θ) measurement (Fig. 2) can indicate significant differences with respect to effusion cell temperatures, those differences came from not the crystallinity of films but the distribution of ZnSe (111) plane around ψ-axis.

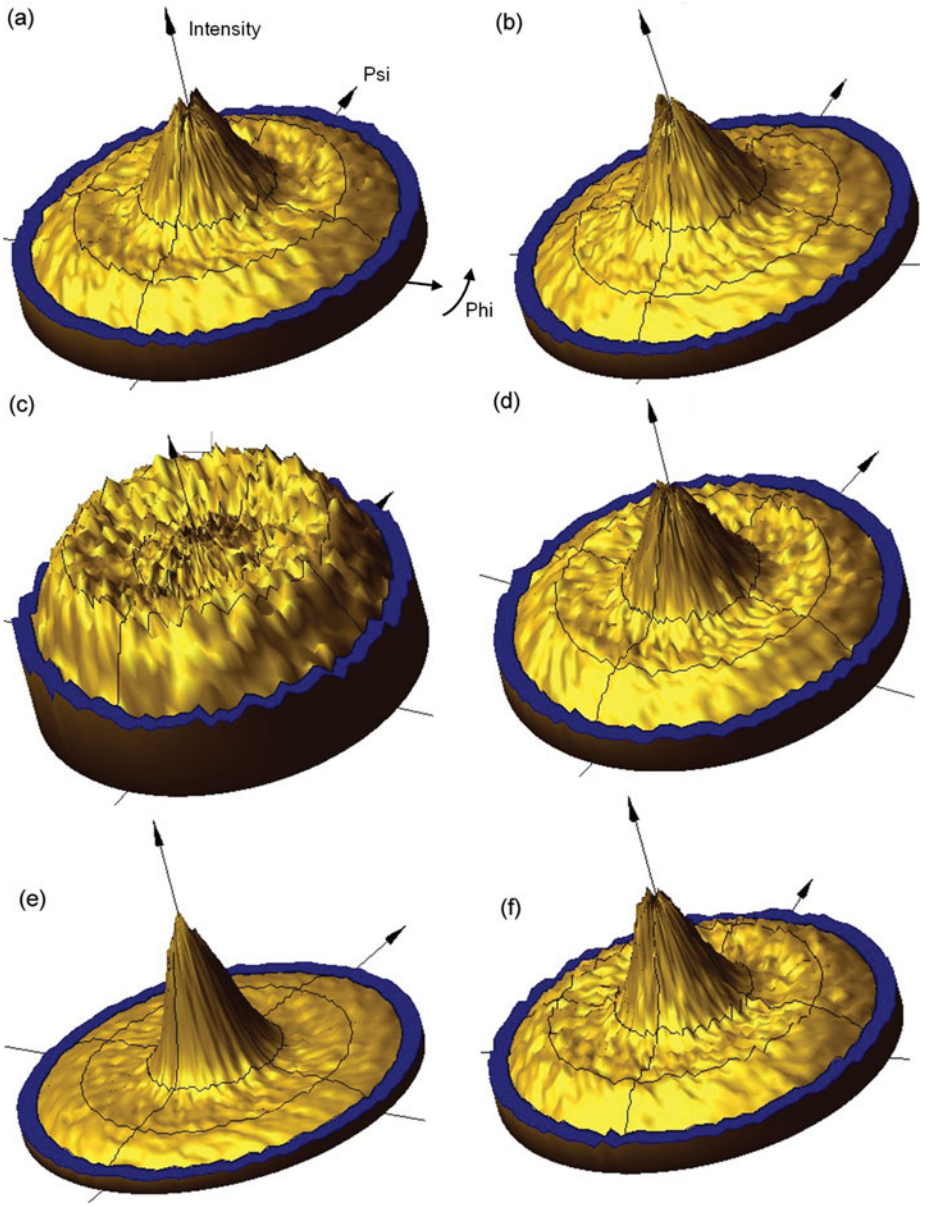

Figure 3. XRD Pole-figures of ZnSe thin films at the cubic (111) plane measured at several selenium effusion cell temperatures. (a) 100°C, (b) 105°C, (c) 110°C, (d) 115°C, (e) 120°C and (f) 125°C, respectively.

In order to investigate the optical properties of specimens under different effusion cell temperatures, the UV-Vis-Nir transmittance is measured. Figure 6 represents the diffused transmittance measured using the 150 mm integrating sphere. As shown in Fig. 6, apparent transmittance difference was not revealed. We also obtained the optical band-gap information from the transmittance measurements, as listed in Table 3 and the fits of the bandgap determination was exhibited in Fig. 6 for 115°C specimen. From these spectral data, optical

Table 3. The value of the energy bandgap for films deposited at various effusion cell temperatures

	Se Effusion Cell Temperature (°C)					
Condition	100	105	110	115	120	125
Bandgap (eV)	2.65	2.65	2.58	2.63	2.66	2.57

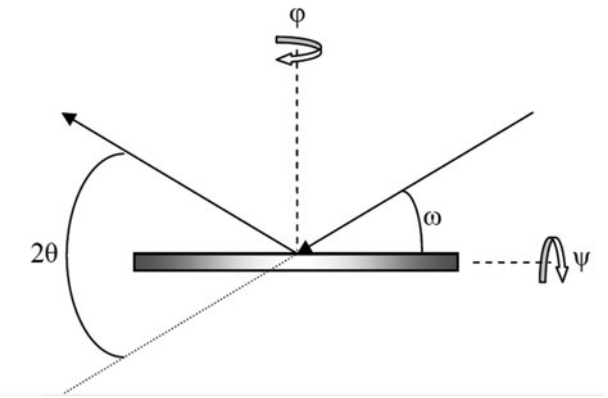

Figure 4. Conventional method of defining the axis of pole-figure measurement in XRD analysis.

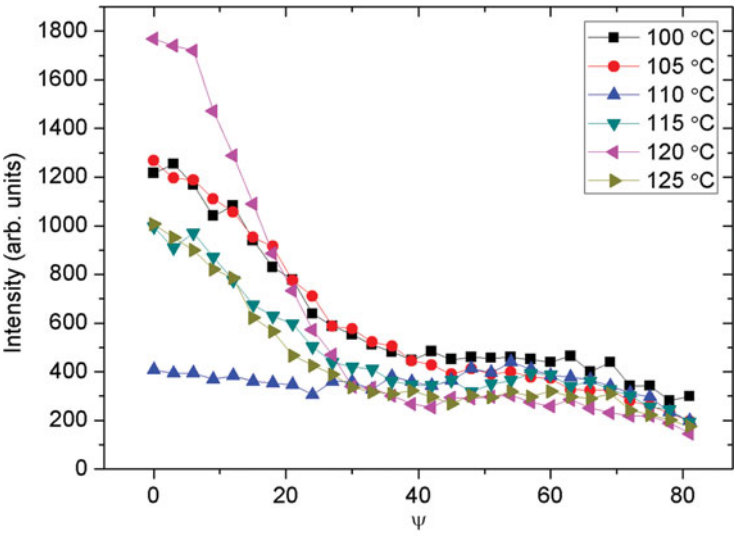

Figure 5. Cross-section of Fig. 3 at $\phi = 24^{\circ}$.

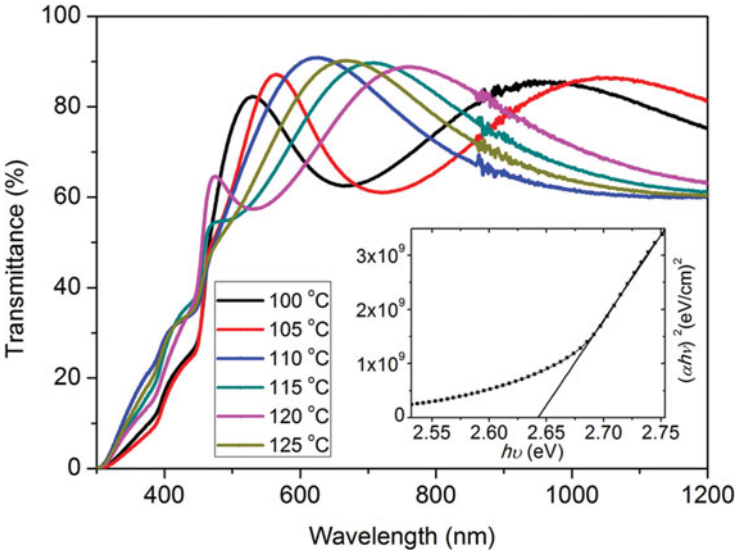

Figure 6. Diffused transmittance using the 150 mm integrating sphere measured at different effusion cell temperatures.

absorption coefficients α were calculated using Lambert's law [11]

$$\mathrm{In}\left(\frac{I_o}{I}\right) = 2.303A = \alpha d \tag{1}$$

Where I_o and I are the intensity of incident and transmitted light, respectively, A is the optical absorbance, and d is the film thickness. Because ZnSe is a direct band-gap (2.7 eV) semiconductor [12], the band gap energy can be calculated from a well-known relation [13]

$$\alpha h\upsilon = \left[k\left(h\upsilon - E_g\right)^{\frac{1}{2}}\right] \tag{2}$$

Where k is a constant, $h\upsilon$ is the photon energy, and E_g is the band-gap energy. For $h\upsilon > 2.7$ eV, the plot of $(\alpha h\upsilon)^2$ as a function of $h\upsilon$ is linear (fundamental absorption). Therefore, in this range the absorption spectrum can be described by Eq. (1). The least-square fit to the linear component gives the optical band gap E_g. The nonlinear steps within the energy range $h\upsilon < 2.7$ eV (residual absorption) can be due to multiple-reflections occurring at the surface and the backside of the film. The value of the energy bandgap estimated from the plots for film deposited at various effusion cell temperatures ranges from 2.57 to 2.66 eV, as shown in Table 3.

Conclusion

In this study, we deposited ZnSe thin films via a co-evaporation method. A comparative study on the optical, structural, and morphological properties of ZnSe films has been performed with respect to various deposition conditions. It has been found that as long as the Se/Zn flux ratio is larger than 1.43, stable, single-phase, ZnSe thin films can be grown. The thickness of ZnSe thin films depending on the effusion cell temperatures are not monotonic behavior due to different surface diagrams. ZnSe (111) plane has various

growth direction with respect to growth conditions. By using this characterization of ZnSe thin films, suitable n type window layer was deposited on the chalcopyrite absorber layer with appropriate deposition conditions.

Acknowledgment

This research was financially supported by the Ministry of Knowledge Economy(MKE), Korea Institute for Advancement of Technology(KIAT) and Dae-Gyeong Leading Industry Office through the Leading Industry Development for Economic Region)

References

[1] Lokhande, C. D., Patil, P. S., Ennaoui, A., & Tributsch, H. (1998). Chemical bath ZnSe thin films: deposition and characterization. *Appl. Surf. Sci.*, *123–124*, pp. 294–297.
[2] Kumaresan, R., Ichimura, M., & Arai, E. (2002). Photochemical deposition of ZnSe polycrystalline thin films and their characterization. *Thin Solid Films*, *414*, pp. 25–30.
[3] Rizzo, A., Tagliente, M. A., Caneve, L., & Scaglione, S. (2000). The influence of the momentum transfer on the structural and optical properties of ZnSe thin films prepared by r.f. magnetron sputtering. *Thin Solid Films*, *368*, pp. 8–14.
[4] Chelvanathan, P., Hossain, M. I., & Amin, N. (2010). Performance analysis of copper–indium–gallium–diselenide (CIGS) solar cells with various buffer layers by SCAPS. *Current Applied Physics*, pp. S387–S391.
[5] Muhammad, H. Asghar, Muhammad, Shoaib, Frank, Placido, & Shahzad, Naseem (2009). Modeling and preparation of practical optical filters. *Current Applied Physics*, *9*, pp. 1046–1053.
[6] Singh, H., Millier, B., Aue, W. A., Riley, J., Wolfframm, D., Evans, A., & Westwood, D. (1996). Studies in the growth of ZnSe on GaAs (001). *Journal of Crystal Growth*, *160*, pp. 193–200.
[7] Farrell, H. H., Tamargo, M. C., Shibli, S. M., & Cheng, Y. (1990). The structure of the ZnSe (100) c(2 × 2) surface. *J Vac Sci Technol*, *B 8*, pp. 884–887.
[8] Riley, J., Wolfframm, D., Westwood, D., & Evans, A. (1996). Surface phase diagram for ZnSe MBE growth. in Proceedings of the optoelectronic and microelectronic materials and devices, pp. 402–405.
[9] Kim, W. K., Payzant, E. A., Kim, S., Speakman, S. A., Crisalle, O. D., & Anderson, T. J. (2008). Reaction kinetics of CuGaSe2 formation from a GaSe/CuSe bilayer precursor film. *Journal of Crystal Growth*, *310*, pp. 2987–2994.
[10] Wolframm, D., Evans, D. A., Westwood, D. I., & Riley, J. (2000). A detailed surface phase diagram for ZnSe MBE growth and ZnSe/GaAs(001) interface studies. *Journal of Crystal Growth 216*, pp. 119–126.
[11] Adachi, A., Kudo, A., & Sakata, T. (1995). The Optical and Photoelectrochemical Properties of Electrodeposited CdS and SnS Thin Films. *Bull. Chem. Soc. Jpn.*, *68*, pp. 3283.
[12] Gudage, Y. G., Deshpande, N. G., Sagade, Abhay A., & Sharma, Ramphal (2009). Room temperature electrosynthesis of ZnSe. *Journal of Alloys and Compounds*, *488*, pp. 157–162.
[13] Pankove, J. I. (1971). *Optical Processes in Semiconductors*, Prentice-Hall, Englewood Cliffs, NJ.